Author/s:
Bradley, SJ;Chi, M;White, JM;Hall, CR;Goerigk, L;Smith, TA;Ghiggino, KP

Title:
The role of conformational heterogeneity in the excited state dynamics of linked diketopyrrolopyrrole dimers

Date:
2021-04-21

Citation:
Bradley, S. J., Chi, M., White, J. M., Hall, C. R., Goerigk, L., Smith, T. A. & Ghiggino, K. P. (2021). The role of conformational heterogeneity in the excited state dynamics of linked diketopyrrolopyrrole dimers. Physical Chemistry Chemical Physics, 23 (15), pp.9357-9364. https://doi.org/10.1039/d1cp00541c.

Persistent Link:
https://hdl.handle.net/11343/280080

PCCP
Physical Chemistry Chemical Physics

Accepted Manuscript

This article can be cited before page numbers have been issued, to do this please use: S. Bradley, M. Chi, J. White, C. R. Hall, L. Goerigk, T. Smith and K. Ghiggino, *Phys. Chem. Chem. Phys.*, 2021, DOI: 10.1039/D1CP00541C.

View Article Online
DOI: 10.1039/D1CP00541C

PCCP

ARTICLE TYPE

Cite this: DOI: 00.0000/xxxxxxxxxx

The role of conformational heterogeneity in the excited state dynamics of linked diketopyrrolopyrrole dimers

Siobhan J. Bradley,[ab] Ming Chi,[a] Jonathan M. White,[a] Christopher R. Hall,[ab] Lars Goerigk,[a] Trevor A. Smith[ab] and Kenneth P. Ghiggino*[ab]

Received Date
Accepted Date

DOI: 00.0000/xxxxxxxxxx

Diketopyrrolopyrrole (DPP) derivatives have been proposed for both singlet fission and energy upconversion as they meet the energetic requirements and exhibit superior photostability compared to many other chromophores. In this study, both time-resolved electronic and IR spectroscopy have been applied to investigate excited state relaxation processes competing with fission in dimers of DPP derivatives with varying linker structures. A charge-separated (CS) state is shown to be an important intermediate with dynamics that are both solvent and linker dependent. The CS state is found for a subset of the total population of excited molecules and it is proposed that CS state formation requires suitably aligned dimers within a broader distribution of conformations available in solution. No long-lived triplet signatures indicative of singlet fission were detected, with the CS state likely acting as an alternative relaxation pathway for the excitation energy. This study provides insight into the role of molecular conformation in determining excited state relaxation pathways in DPP dimer systems.

1 Introduction

Photophysical studies of covalently linked chromophores in solution have the potential to provide additional insight into the factors that govern singlet fission which cannot be elucidated from solid-state studies. By studying isolated bichromophoric molecules in solution rather than thin films of stacked chromophores, complex intermolecular interactions and structural heterogeneity unique to crystalline and solid state structures can be eliminated allowing the study of the minimum possible unit of singlet fission.[1–5] One can also study the role of charge-transfer (CT) states through variation of the solvent dielectric constant.[6–9] However, in the absence of the rigid thin-film packing environment, the flexibility of molecular conformation in solution can add a level of complexity. Only a limited number of chromophores have been investigated in linked dimers in order to understand the process of singlet fission. Exothermic systems have received particular attention as the excess energy ($ES_1 > 2(ET_1)$) allows a certain degree of energetic flexibility, for example, if singlet or triplet energy levels are perturbed when chromophores come in close proximity, adopting different conformations in a thin-film environment.[1,4,10,11] Diketopyrrolopyrrole (DPP) is a biradicaloid molecule, a feature which allows for a suitably low triplet energy thus making singlet fission energetically feasible in some derivatives such as 3,6-di(thiophen-2yl)diketopyrrolopyrrole (TDPP). DPP derivatives have strong charge-transfer character along with high emission quantum yield and photostability, and have been shown to undergo efficient singlet fission in thin films.[12–15] However identifying intramolecular singlet fission in dimers of DPP derivatives is less straightforward compared with non-linked equivalent systems, due to two main factors. Firstly, it has been shown in previous work that the spectral features of the key excited state species - the charge-transfer state, correlated triplet pair and isolated triplet - overlap strongly.[16–18] Secondly, the ability of the DPP chromophore to accommodate charge - to form charge-transfer and charge separated species - necessitates methods to deconvolve the competing photophysical pathways. Despite these challenges, singlet-fission has been recently reported in a study of DPP dimers linked via a dithienylphenylene spacer at the ortho, meta or para positions.[19] That study suggests that some charge-transfer character facilitates singlet fission in DPP - as seen in the ortho and meta dimers in polar solvents. However, very strong charge-transfer character as observed in the para form of the dimer can lead to symmetry-breaking charge separation (SBCS), which acts as a trap. In another DPP dimer study, Mauck and co-workers studied DPP chro-

[a] School of Chemistry, University of Melbourne, Melbourne, Australia. Fax: +61 3 9347 5180; Tel: +61 3 8344 8939; E-mail: ghiggino@unimelb.edu.au
[b] ARC Centre of Excellence in Exciton Science, University of Melbourne, Melbourne, Australia.

† Electronic Supplementary Information (ESI) available: [details of any supplementary information available should be included here]. See DOI: 10.1039/cXCP00000x/

View Article Online
DOI: 10.1039/D1CP00541C

mophores coupled via a xanthene linker to mimic $\pi - \pi$ stacking seen in thin films which was previously reported to show efficient singlet fission.[16] These authors proposed a pseudoequilibrium model where the S_1S_0 state can reach a relaxed S_1S_0' state via the charge transfer state or, in polar solvents can form the fully charge-separated ion pair state. In either case, the intermediate states observed provided an alternative relaxation pathway to singlet fission. These studies highlight the complexity of the charged intermediate states competing with the singlet fission pathway in DPP derivatives necessitating further investigation. In this study, dimers of TDPP have been designed with varying linker flexibility to study the effect of dimer geometry, and thus coupling, on the excited state relaxation processes. For simplicity we henceforth refer to these TDPP derivates as "DPP". The molecules under investigation are given in Figure 1. Three dimers were synthesised -

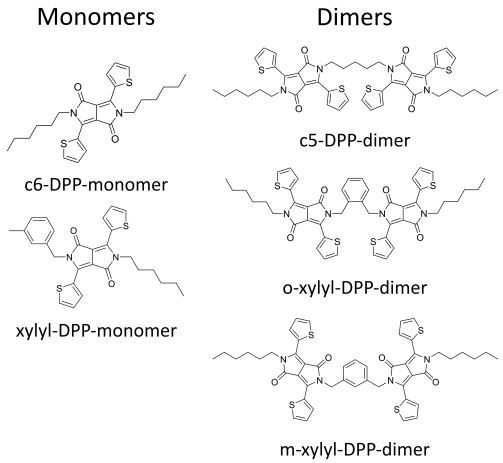

Fig. 1 Structures of the DPP derivatives investigated in this work.

one with a flexible saturated five carbon linker (c5-DPP) and two dimers coupled via a more rigid xylyl linker, one coupled at the meta (m-xylyl DPP) and the other at the ortho (o-xylyl DPP) position. The corresponding monomers were also synthesised as reference materials. Both electronic and IR transient spectroscopy were used to study the photophysics of the dimers in solvents of varying dielectric constant in order to understand the role of molecular conformation and electronic coupling on excited state relaxation mechanisms.

2 Experimental

2.1 Materials

Unless stated otherwise all chemicals and solvents were purchased from Sigma-Aldrich or Merck and used as received. Detailed descriptions of the synthetic methods for model and dimer compounds are given in the ESI†.

2.2 Computational Details

Conformational pre-screenings of ground-state geometries of the c5- and m-xylyl DPP dimers were conducted with the efficient semi-empirical molecular-orbital model GFN2-xTB[20] - using Grimme's standalone program[21] - yielding up to nearly 150 conformers in some cases. GFN2-xTB's own implicit-solvation model was used for this purpose. Further refinement of the geometries was achieved at the B97-3c[22] level of theory, which is an efficient low-cost DFT method, that takes into account crucial London-dispersion effects and minimizes basis-set incompletion errors by using its own triple-ζ atomic-orbital (AO) basis set. The conductor-like screening model (COSMO)[23] was used to incorporate solvation effects. B97-3c calculations were carried out with TURBOMOLE 7.4.1,[24] its numerical integration grid "m4", and the resolution-of-the-identity (RI) approximation to the Coulomb integrals using the appropriate auxiliary basis set.[25] The most stable conformers within a 5 kcal/mol window (6 kcal/mol for the m-xylyl DPP dimer) and the fully extended conformers were then used for single-point calculations to obtain accurate relative energies. For this purpose, we used the range-separated, dispersion-corrected double-hybrid ω-B97X-2[26]-D3(BJ[27–29]) in its "TQZ" parametrization in conjunction with the def2-TZVPP[30] triple-ζ AO basis set. This functional has been shown to be one of the most accurate and robust to treat relative energies in conformers based on the comprehensive GMTKN55[31] database for general main-group chemistry, kinetics, and noncovalent interactions[29]. A local version of ORCA4[32] was used for these calculations. ORCA's grid "4" and the conductor-like polarizable continuum model[33] (CPCM) were applied in all cases. The perturbative part of the double-hybrid functional was calculated within the RI approximation with an appropriate auxiliary basis set.[34] Self-consistent-field convergence criteria were set to 10^{-7} E_h in all TURBOMOLE and ORCA calculations. The geometry convergence criterion was set to 10^{-7} E_h with respect to the change in total energy between two optimization cycles.

2.3 Photophysical Characterisation (Steady-State)

The UV-vis absorption spectra of all samples were acquired using a UV-visible spectrophotometer (CARY 50 Bio, Varian). Steady-state PL spectra were acquired on a Varian Eclipse spectrofluorimeter using an excitation wavelength of 525 nm and excitation and emission bandwidths set to 5 nm.

2.4 Photophysical Characterisation (Time-Resolved)

2.4.1 TCSPC

Solution samples were excited with a mode-locked and cavity-dumped Ti/sapphire laser (Coherent Mira 900F/APE PulseSwitch) pumped by a Coherent Verdi-10 DPSS Nd:YVO_4 laser. The laser output (800 nm wavelength, 5.4 MHz repetition rate) was frequency-doubled to provide an excitation wavelength of 400 nm. The individual fluorescence decay curves were collected using an f1 lens after first passing through an emission polarisation analyser set at the magic angle, then a monochromator (Jobin Yvon H20) and detected using a hybrid photomultiplier tube (Becker & Hickl, HPM100) fed to a time-correlated single photon counting (TCSPC) module (SPC-150, Becker & Hickl, Berlin, Germany). The fluorescence decay times were extracted from the decay profiles using nonlinear least square iterative reconvolution software (FAST, Edinburgh Instruments Ltd) and a sum-of-exponentials analysis.

View Article Online
DOI: 10.1039/D1CP00541C

2.4.2 Transient Absorption Spectroscopy

Femtosecond transient absorption measurements were performed using a pump-probe configuration based on a high repetition rate (96 kHz, 60 fs) Coherent RegA 9050 amplifier. Pulses of 800 nm were split and passed through a tunable optical parametric amplifier (Coherent OPA 9450) on one arm to generate the pump (505 nm) beam while the other arm generated the white light continuum probe beam using a 3 mm-thick sapphire window (CASTECH). An off-axis parabolic reflector focused the pump and probe pulses to overlap in the solution-phase sample with a pump spot size of approximately 200 μm, giving an excitation fluence of 0.80 μJ cm^{-2}. Pump-induced absorption changes (ΔOD) of the solutions in a 2 mm pathlength optical cell were measured by comparing adjacent transmitted probe pulses with and without pump pulses using a synchronized mechanical chopper in the path of the pump beam. The time-resolved transient absorption spectra were recorded using a high-speed fibre-optic spectrometer (Ultrafast Systems) at ~7.4 kHz. The instrument response function was estimated to be ca. 150 fs FWHM.

2.4.3 Transient Infrared Spectroscopy

The transient infrared spectroscopy measurements were performed on the ULTRA spectroscopy platform at the Central Laser Facility (CLF) at the Rutherford Appleton Laboratory (RAL) at Harwell, UK. The excitation pulses had a central wavelength of 450 nm, a duration of 100 fs and a pulse energy of 1μJ. The pulses were focused to a 100 μm diameter spot. The excited region is probed by broadband (~300 cm^{-1}) infrared probe pulses. Both pump and probe pulses are generated at a repetition rate of 10 kHz, with every second pump pulse chopped by a fast optical chopper, reducing the excitation rate to 5 kHz. Probe transmission through the sample was recorded alternately in the presence and absence of the pump pulse to generate the transient difference spectrum. The samples had an optical density of 0.1-0.2 in a 50 μm pathlength demountable liquid cell (Harrick Scientific). The sample cell was rapidly raster scanned around the focal spot region over the course of the measurement to refresh the sample within the excitation spot.

2.5 Global analysis

The GloTarAn Analysis Program[35] was used to decompose the large multidimensional transient absorption and transient infrared datasets to determine the principal states involved in the photophysical relaxation pathways of the molecules under investigation. A target model was tested which describes the dynamics of the concentrations of the various excited-state species. We used a branched model to describe the subpopulations of DPP dimer molecules. Further information on the model description and application are given in the ESI†.

3 Results and Discussion

3.1 Synthesis

Full details of the monomer and dimer synthetic procedures can be found in the ESI(Figures S1 - S6†). ^{1}H NMR spectra showing no significant contribution from impurities are given in Figures S7-S11†.

3.2 Computational Analysis

A conformational analysis of the c5-DPP and m-xylyl-DPP dimers in a toluene and DMSO solvent continuum was performed to illustrate the effect of solvent and linker on the ground state conformations. The ground state dimer configurations are relevant as they provide an insight into the initial conformations being excited before any excited state rearrangements can occur. Currently, there are no efficient methods available that allow the sampling of conformers of large, flexible systems for excited states. The four lowest energy conformations of the c5-DPP and m-xylyl DPP dimers in each solvent are given in Figure 2a. The results of our calculations suggest that the dimers exist in a folded conformation in the ground state. For the m-xylyl dimer, we calculated fewer low energy conformations than for the c5-dimer and there is a stronger weighting towards the lowest energy, folded structure (see Table S1†). The energy of the fully extended conformation of the c5-dimer, where the two chromophores are non-interacting, was calculated to be thermally inaccessible (Figure S12†) with an energy difference of about 20 kcal/mol relative to the most stable conformer depending on the solvent (see Table S1†). This contrasts with an earlier study using lower levels of theory reporting a DPP dimer in a fully extended conformation which folds in the excited state.[36] The calculations also show a minor slip angle between the chromophores and misalignment of transition dipole moments of the chromophores (Figures 2a and b, respectively).

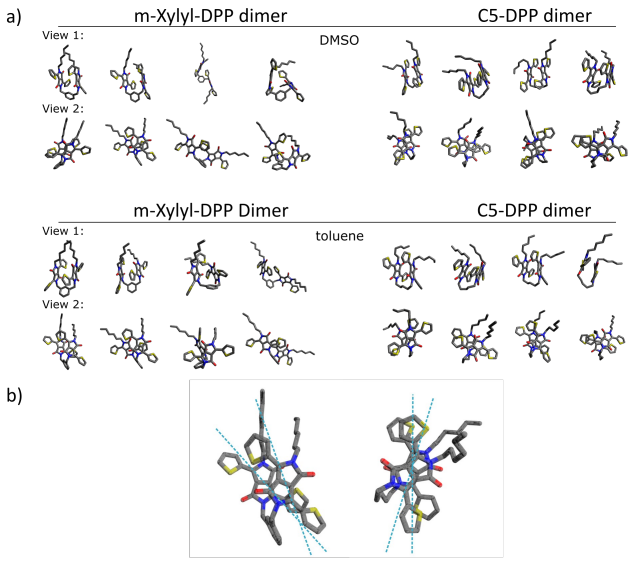

Fig. 2 a) Ground state calculated structures (B97-3c(COSMO) level of theory[22,23]) of the four lowest energy c5-DPP dimer and m-xylyl-DPP dimer conformers in solvents as indicated. The chromophores are shown side-on in view 1 and face-on in view 2. b) The lowest energy structures of the c5-dimer and m-xylyl dimer in DMSO with the direction of the transition dipole moments indicated by the blue dashed line (as previously reported.[37])

These two factors were shown previously to be important for singlet fission in DPP molecules.[14] The minimum interchro-

View Article Online
DOI: 10.1039/D1CP00541C

mophore distances were approximately 3.5 Å for each folded derivative in each solvent (see ESI†). A list of the energies of all calculated structures is given in Table S1†.

3.3 Photophysical Characterisation

3.3.1 Steady-State Characterisation

The steady-state absorption and emission spectra of the DPP dimers showed high similarity to their monomer model compounds (see Figure S13†). One exception of note is the meta-xylyl DPP dimer which shows a significant reversal of the vibronic peak height ratios in DMSO compared to toluene and the monomer model suggesting proximity and thus some coupling between the dimer chromophores (Figure 3a).

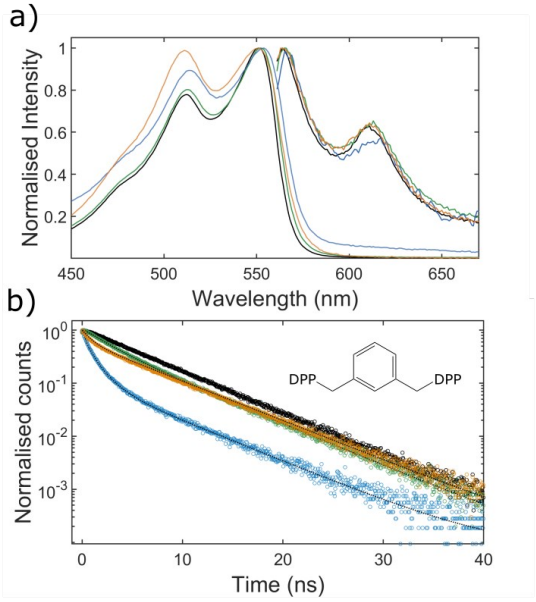

Fig. 3 a) Steady-state absorption (left) and emission (right) spectra of the m-xylyl-DPP dimer showing the change in vibronic band intensity with solvent (toluene = green, benzonitrile = blue, DMSO = gold and benzyl monomer control in toluene in black). b) Fluorescence decay curves of the same dimer in toluene, benzonitrile, DMSO (colour scheme as in (a)) showing an additional shorter component present in polar solvents (monomer control in black for comparison).

Similar behaviour has been seen in a previous DPP dimer study and attributed to increased coupling between the chromophores.[16] This indicates the linker can moderate the conformations the dimers can adopt, as this behaviour is not as evident in the flexible c5-DPP or o-xylyl-DPP dimers.

3.3.2 Time-Resolved Fluorescence Measurements

Time-resolved fluorescence (TRF) measurements were performed to investigate the excited-state dynamics of the DPP samples. Plots of the TRF data for all DPP dimers and controls are given in Figure S14† with fit parameters given in Table S2†. The decays of the monomers and dimers in non-polar toluene generally can be fit with a single exponential model with lifetimes between 5 and 6 ns, indicative of similar relaxation pathways for both systems. For all dimers in polar solvents, as shown for the m-xylyl DPP dimer in Figure 3b, an additional, faster component is present which is not observed in the monomers. For all dimers in polar solvents, a sum of exponentials decay function was required to adequately fit the data (see Figure S14† and Table 1). The existence of a monomer-like component (~5-6 ns) in each dimer decay along with shorter decay components suggests multiple subpopulations of dimers in solution are being excited (i.e. subpopulation 1 relaxes as isolated monomers while subpopulation 2 has additional faster relaxation pathways). The m-xylyl-DPP dimer exhibits two interesting exceptions to the aforementioned trend (Figure 3b and Table S2†). Firstly, this dimer shows biexponential fluorescence decay in toluene that is not observed in the monomer, and secondly, it shows triexponential decay in benzonitrile. This triexponential decay suggests two alternative pathways for quenching and therefore three subpopulations in total.

3.3.3 Transient absorption spectroscopy

Femtosecond Transient Absorption Spectroscopy (TAS) was used to further investigate the excited state species involved in the relaxation of the DPP dimers. The DPP monomers have similar transient spectral features to previously reported monomeric DPP derivatives (Figures S15 and S16†).[16,19,36] The main ground state bleach is seen in the wavelength range 460 - 600 nm which matches the absorption spectrum, and stimulated emission is observed from 600 nm to 675 nm matching the fluorescence spectrum of the monomer. A $S_1 \rightarrow S_n$ broad absorption band appears at longer wavelengths (675 - 800 nm). Similar spectral features are observed in c5-DPP and o-xylyl-DPP in non-polar toluene. In the dimer transient absorption spectra, we did not observe photophysical behaviour consistent with singlet fission i.e. fast formation of a triplet state with positive features in the range 580-600 nm and negative features either side which persists beyond the 8 ns time window of our experiment.[14,15] Instead, we observed an excited state absorption (ESA) unique to the DPP dimers which grows in at 640 nm in polar solvents (Figure 4a and Figures S17 - S19†). This feature is not observed in the monomer model compounds. This ESA grows in at a rate which is dependent on both solvent and linker structure. The solvent-dependent nature of this species along with previous studies on charge-transfer and charge-separated states in DPP derivatives allows us to assign this species as the radical anion of a charge-separated state.[16,38,39] Indeed, spectro-electrochemical studies show that this absorption can be induced by applying a negative potential (Figure S20†).

Global analysis using GloTarAn target analysis software was performed on the transient absorption data to decompose the spectra and determine the main species involved in the relaxation pathways.[35] For the dimer-solvent combinations showing biexponential fluorescence decays, a kinetic model is proposed where excitation of two main subpopulations of dimer conformers in solution gives rise to distinct S_1S_0 states (Figure 5). The pre-exponential factors from the fit to the fluorescence decays were used to fix the branching ratio in the model.

Subpopulation 1, represented by species-associated spectrum 1 in blue (Figure 4c), relaxes to the ground state radiatively and non-radiatively with a similar rate to the corresponding monomer control. This lifetime was fixed to the long lifetime of the fit to

View Article Online
DOI: 10.1039/D1CP00541C

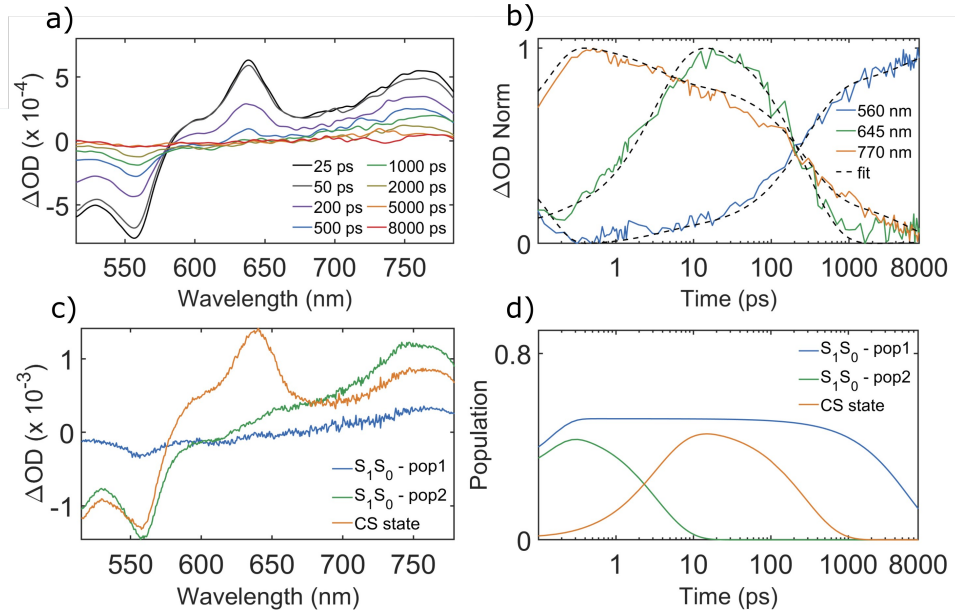

Fig. 4 a) Femtosecond transient absorption spectra of m-xylyl DPP dimer in DMSO (pump 505 nm). b) Temporal profiles of key transient features at wavelengths labelled with the global fit overlayed (dashed line). c) Species associated spectra from the global fit using the kinetic model given in Figure 5 labelled as singlet population 1 in blue, singlet population 2 in green and CS state in gold. d) Population kinetics of species in (c).

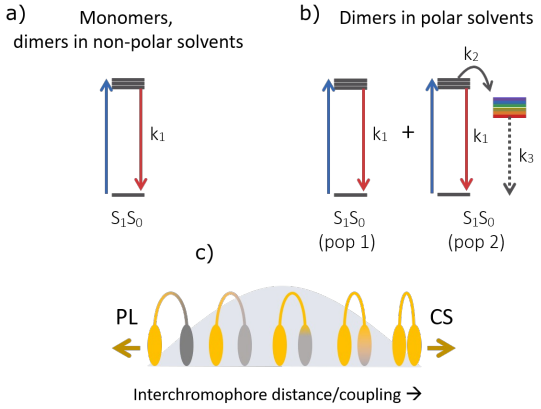

Fig. 5 Kinetic scheme used in the global analysis of the DPP dimer transient absorption datasets. a) For model compounds in all solvents and the dimers in non-polar solvents, the excited molecules relax via a first order (sum of radiative and non-radiative) process. b) For dimers in polar solvents, there are two main subpopulations with different conformations. In one subpopulation the chromophores are sufficiently distanced that they relax like the model compounds. In the second subpopulation where chromophores are closer together and suitably aligned, the main relaxation pathway is via the charge-separated state. c) Graphical representation of the effect of interchromophore distance (in different molecular conformations) on the relaxation pathways taken.

the fluorescence decay. Superimposed on this behaviour is that of subpopulation 2 (SAS 2 in green) which relaxes non-radiatively via the charge-separated state (SAS 3 in gold). The proportion of this second population of S_1S_0, along with the rate of formation and decay of the charge-separated state, is affected by both the linker structure and the solvent dielectric constant. The global fit to our proposed model shows two species with spectral features similar to the monomer transient absorption spectrum and a third species with charge-separated state absorption around 640 nm. In the o-xylyl and m-xylyl DPP dimers the CS state forms faster in DMSO but in higher abundance in benzonitrile, as determined from the preexponential factors, indicating the proportion of the total TCSPC signal amplitude (Table 1).

This suggests that solvent polarity alone does not drive the formation of the CS state but rather the solvent affects the molecular conformation which in turn tunes the interchromophore distance and thus orbital overlap determining the rate of formation and total population of the excited state. The m-xylyl-DPP dimer in benzonitrile - which had a triexponential fluorescence decay - could not be adequately fit using this model. The addition of a third step - a conversion between the two populations (S_1S_0 pop1 and pop2) did not lead to a reasonable fit. We therefore suggest that this dimer in benzonitrile can adopt many conformations and that results in complex photophysical behaviour that cannot be adequately fit to the target kinetic model. Although there is evidence of an excited state absorption in the vicinity of the CS state at 640 nm for both c5-DPP dimer in benzonitrile and m-xylyl DPP dimer in toluene, the feature forms at a much slower rate and could not be fully resolved with the experimental time window (~8 ns) available to us. However, this process likely accounts for the non-single exponential fluorescence decays observed in these solvents.

3.3.4 Transient Infrared Spectroscopy

Femtosecond transient infrared spectroscopy was performed on the c5-DPP and m-xylyl-DPP dimers in toluene and DMSO and the data were globally analysed using the model proposed in Figure 5. From previous studies of the ground state IR spectra of DPP molecules, the spectral features of the ground state molecules include an amide carbonyl in the range 1650-1700 cm^{-1}, DPP core aromatic C=C stretches around 1550 cm^{-1} and lower energy

View Article Online
DOI: 10.1039/D1CP00541C

Table 1 Comparison of decay times from the global analysis of the transient absorption of DPP dimers and those derived from the multiexponential fit to the equivalent fluorescence decays where $\tau_{1,2,3} = 1/k_{1,2,3}$. B_i indicates the proportion of the total signal amplitude. Note that τ_1 of the global TA fit was fixed to the long lifetime from the TCSPC results

		τ_{TA}, (ps)			τ_{TCSPC}, (ps) (B_i%)	
Solvent	Derivative	τ_1	τ_2	τ_3	τ_1	τ_2
DMSO	c5-DPP	6061	5.91	714	1150 (43%)	6069 (57%)
	o-DPP	5464	68	456	540 (85%)	5468 (15%)
	m-DPP	5882	3.34	277	884 (48%)	5830 (52%)
bn	o-DPP	5208	457	1457	922 (85%)	5213 (15%)

thiophene aromatic C=C stretches around 1400 cm^{-1}.[39,40] The two strongest bleach transients are common to all DPP derivatives and are found at 1565 cm^{-1} and 1670 cm^{-1} and can be assigned to the C=C out-of-phase stretch of the DPP core and the amide carbonyl of the DPP core respectively (see Figure 6).

A key excited state absorption mode is found at 1520 cm^{-1}. This mode grows in over the 3 ns experimental window in the dimer samples. The mode grows in faster in DMSO than in toluene for both the dimers studied. The c5-dimer transient IR spectra were fit globally using the branched model proposed in Figure 5. The resulting species-associated spectra and population kinetics for the meta-xylyl- and c5-dimer are given in Figure 7.

The relaxation rate of the first population of S_1S_0 was fixed using the fluorescence lifetime value of the corresponding monomer and the other rates were allowed to float. The fit produces rates consistent with the equivalent fit to the transient absorption data (see Table 2). The agreement between the transient lifetimes extracted from global analysis of the TA and TRIR data provides support for the model proposed in Figure 5.

Table 2 Comparison of lifetimes from global analysis of transient absorption and transient IR datasets. Note τ_1 unit is nanoseconds and is fixed to the long fluorescence lifetime

Derivative	Dataset	τ_1 (ns)	τ_2 (ps)	τ_3 (ps)
m-DPP	TA	5.9	3.3	277
	TRIR	5.9	4.7	290
c5-DPP	TA	6.1	5.9	591
	TRIR	6.1	4.4	617

The dominant differences between the two populations of conformers as seen in the species associated spectra are the presence of the mode at 1520 cm^{-1} for the second population of S_1S_0 and the charge separated state only (Figure 7a and c). Given the dynamics of this mode match those of the previously assigned charge-separated species, it is clearly reporting on the dynamics of the charge separated state. The bleach of the amide carbonyl of the DPP core near 1660 cm^{-1} is also shifted to a higher frequency by 3 cm^{-1} in these species and the bleach at 1565 cm^{-1} is more dominant than for the first population of S_1S_0. The higher frequency of the NC=O bleach indicates a strengthening of this bond which could be the result of increased orbital overlap between two closely interacting chromophores.

Recent reports on bichromophoric dimers of sufficient conformational flexibility systematically showed that symmetry breaking charge separation or singlet fission could be tuned through both conformational restrictions and the local solvent environment.[41,42] In the DPP dimer systems under investigation here, the coexistence of faster relaxation pathways with the monomer-like fluorescence reveals underlying dimer subpopulations. We observe mixed spectra comprising contributions from multiple subpopulations of dimers with differing geometries in the steady-state emission, time-resolved fluorescence decays and transient absorption and infrared results. At one extreme, the chromophores of the dimer are sufficiently far apart to exclude any strong electronic coupling between chromophores. In that case, following photoexcitation, a single chromophore is excited and relaxes radiatively in a similar fashion to the model monomer compounds. At the other extreme, the chromophores are sufficiently close and in a geometry favourable to allow orbital overlap between chromophores. The coupling between the chromophores opens up a new non-radiative relaxation pathway via symmetry breaking charge separation. This behaviour is observed in the dimers in polar solvents (benzonitrile and DMSO) and the m-xylyl DPP dimer in toluene suggesting that a combination of bridging unit and solvent properties determines the proportion of molecules with the required geometry for charge separation and the speed at which this process can occur. The role of solvent is more complex than involving dielectric properties alone. DMSO is the most polar solvent used here, however, in general, benzonitrile leads to the faster charge separation and more fluorescence quenching indicating that other properties of the solvent (e.g. aromaticity, specific solute-solvent interactions) may also play a role in the conformation adopted by the dimers allowing the chromophores to come closer together. It has been found that in the case of DPP, SF is close to isoergic and thus, interchromophore interaction can have a significant effect on the energetics of the chromophores compared with isolated model compounds.[43,44] In comparison with earlier reports on covalent DPP dimers, the flexible, unconjugated nature of the bridging unit in our structures involves through-space rather than through-bond coupling, which should be closer to the types of interactions that govern singlet fission in thin films. A number of studies of singlet fission in solid-state DPP systems show that a slip-stacked arrangement of the interacting chromophores is a prerequisite for singlet fission. The bridging structures in this study do not facilitate such a slip-stacked arrangement allowing the charge separation process to dominate, acting as a trap and preventing fission. Finally it should be noted the lower entropy of singlet fission of a bichromophoric dimer system will also play a role in the reduced likelihood for SF compared to the situation in the stacked crystalline material.[11]

View Article Online
DOI: 10.1039/D1CP00541C

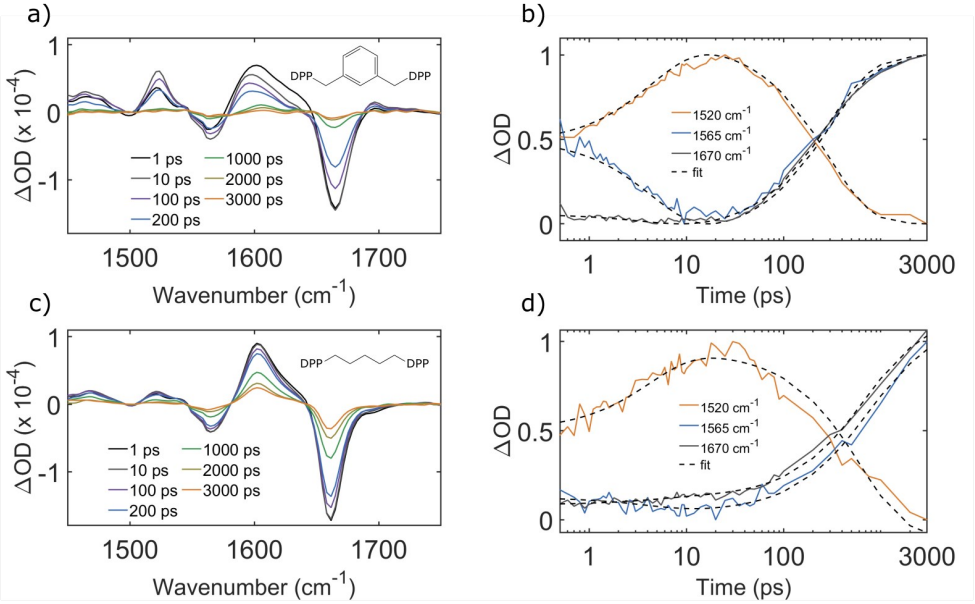

Fig. 6 Transient IR spectra of DPP dimers in DMSO at fixed pump-probe delays and dynamics at fixed frequencies as noted. a,c) Transient IR spectra of the m-xylyl DPP dimer and c5-dimer respectively. b,d) Corresponding temporal evolution at fixed frequencies as indicated. Note the growth of a key excited state feature at 1520 cm^{-1} in gold. The dashed line gives the fit from the proposed kinetic model.

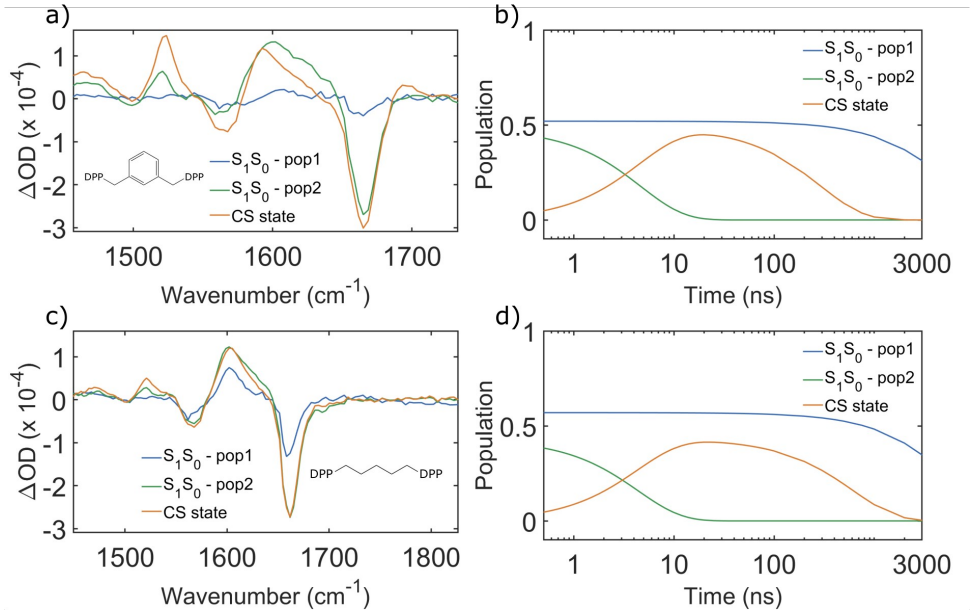

Fig. 7 Species-associated spectra of m-xylyl and c5-dimer in DMSO from a global fit to the transient-IR spectra using the kinetic scheme given in Figure 5.

4 Conclusions

Flexibly linked DPP dimers were investigated to determine the role of dimer geometry on their excited-state relaxation processes. Dispersion-corrected DFT calculations, along with steady state spectroscopy, time-resolved fluorescence and transient electronic and IR spectroscopies revealed the existence of multiple subpopulations of folded conformers contributing to their ultrafast dynamics. While a flexible bridge eliminated complicating through-bond interactions, we found that the added flexibility allowed for conformational heterogeneity which resulted in complex photophysical behaviour. A new model for DPP-dimers is used to explain the observed results where two main subpopulations of molecular conformers relax to the ground state via parallel pathways. One subpopulation exists in a conformation where there is interaction between chromophores leading to charge-separated state formation. We have found the solvent not only modifies the dielectric environment but also plays an additional role affecting the conformations available to the molecule and thus the yield of the charge-separated state. Other work has highlighted the effect of interchromophore distance and orientation on the coupling of

View Article Online
DOI: 10.1039/D1CP00541C

pentacenes which affects the formation of the correlated triplet pair and resulting rate of singlet fission.[45] We see no evidence suggesting the formation of a correlated triplet pair or recombination in our system. We conclude that the linker flexibility, rather than allowing the dimers to adopt a favourable geometry for singlet fission, allowed a more complex distribution of molecular conformers which lead to relaxation via several competing pathways. This study highlights the important role of conformational heterogeneity in the photophysics of linked DPP dimers.

Conflicts of interest

There are no conflicts to declare.

Acknowledgements

The authors would like to thank Steve Meech, Greg Greetham, Ian Clark, James Iuliano and Jinnette Tolentino Collado for assistance with TIR measurements at the Rutherford Appleton Laboratory. L. G. acknowledges generous allocations of computational resources from the National Computational Infrastructure (NCI) Facility within the National Computational Merit Allocation Scheme (project fk5), and Research Platform Services (ResPlat) at The University of Melbourne (project punim0094). This work was supported by the Australian Research Council through the Centre of Excellence in Exciton Science (CE170100026) and grant LE200100051.

Notes and references

1 M. Kasha, H. R. Rawls and M. A. El-Bayoumi, *Pure and Applied Chemistry*, 1965, **11**, 371–392.
2 J. C. Johnson, A. J. Nozik and J. Michl, *Acc. Chem. Res.*, 2013, **46**, 1290–1299.
3 S. N. Sanders, E. Kumarasamy, A. B. Pun, M. T. Trinh, B. Choi, J. Xia, E. J. Taffet, J. Z. Low, J. R. Miller, X. Roy, X.-Y. Zhu, M. L. Steigerwald, M. Y. Sfeir and L. M. Campos, *J. Am. Chem. Soc.*, 2015, **137**, 8965–8972.
4 C. Hetzer, D. M. Guldi and R. R. Tykwinski, *Chemistry – A European Journal*, 2018, **24**, 8245–8257.
5 N. V. Korovina, N. F. Pompetti and J. C. Johnson, *J. Chem. Phys.*, 2020, **152**, 040904.
6 S. Lukman, K. Chen, J. M. Hodgkiss, D. H. P. Turban, N. D. M. Hine, S. Dong, J. Wu, N. C. Greenham and A. J. Musser, *Nature Communications*, 2016, **7**, 13622.
7 N. Monahan and X.-Y. Zhu, *Annual Review of Physical Chemistry*, 2015, **66**, 601–618.
8 B. S. Basel, J. Zirzlmeier, C. Hetzer, S. R. Reddy, B. T. Phelan, M. D. Krzyaniak, M. K. Volland, P. B. Coto, R. M. Young, T. Clark, M. Thoss, R. R. Tykwinski, M. R. Wasielewski and D. M. Guldi, *Chem*, 2018, **4**, 1092–1111.
9 E. A. Margulies, J. L. Logsdon, C. E. Miller, L. Ma, E. Simonoff, R. M. Young, G. C. Schatz and M. R. Wasielewski, *J. Am. Chem. Soc.*, 2017, **139**, 663–671.
10 K. C. Krishnapriya, A. J. Musser and S. Patil, *ACS Energy Lett.*, 2019, **4**, 192–202.
11 W.-L. Chan, M. Ligges and X.-Y. Zhu, *Nature Chemistry*, 2012, **4**, 840–845.
12 M. A. Naik, N. Venkatramaiah, C. Kanimozhi and S. Patil, *J. Phys. Chem. C*, 2012, **116**, 26128–26137.
13 R. S. Szabadai, J. Roth-Barton, K. P. Ghiggino, J. M. White and D. J. D. Wilson, *Aust. J. Chem.*, 2014, **67**, 1330–1337.
14 P. E. Hartnett, E. A. Margulies, C. M. Mauck, S. A. Miller, Y. Wu, Y.-L. Wu, T. J. Marks and M. R. Wasielewski, *J. Phys. Chem. B*, 2016, **120**, 1357–1366.
15 C. M. Mauck, P. E. Hartnett, E. A. Margulies, L. Ma, C. E. Miller, G. C. Schatz, T. J. Marks and M. R. Wasielewski, *J. Am. Chem. Soc.*, 2016, **138**, 11749–11761.
16 C. M. Mauck, Y. J. Bae, M. Chen, N. Powers-Riggs, Y.-L. Wu and M. R. Wasielewski, *ChemPhotoChem*, 2018, **2**, 223–233.
17 C. M. Mauck, P. E. Hartnett, Y.-L. Wu, C. E. Miller, T. J. Marks and M. R. Wasielewski, *Chem. Mater.*, 2017, **29**, 6810–6817.
18 T. Mukhopadhyay, A. J. Musser, B. Puttaraju, J. Dhar, R. H. Friend and S. Patil, *J. Phys. Chem. Lett.*, 2017, **8**, 984–991.
19 I. Papadopoulos, M. J. Álvaro-Martins, D. Molina, P. M. McCosker, P. A. Keller, T. Clark, Á. Sastre-Santos and D. M. Guldi, *Advanced Energy Materials*, 2020, **10**, 2001496.
20 C. Bannwarth, S. Ehlert and S. Grimme, *J. Chem. Theory Comput.*, 2019, **15**, 1652–1671.
21 S. Grimme, *GFN2-xTB*, 2018.
22 J. G. Brandenburg, C. Bannwarth, A. Hansen and S. Grimme, *J. Chem. Phys.*, 2018, **148**, 064104.
23 A. Klamt and G. Schüürmann, *J. Chem. Soc., Perkin Trans. 2*, 1993, 799–805.
24 F. Furche, R. Ahlrichs, C. Hättig, W. Klopper, M. Sierka and F. Weigend, *WIREs Computational Molecular Science*, 2014, **4**, 91–100.
25 K. Eichkorn, F. Weigend, O. Treutler and R. Ahlrichs, *Theor Chem Acta*, 1997, **97**, 119–124.
26 J.-D. Chai and M. Head-Gordon, *J. Chem. Phys.*, 2009, **131**, 174105.
27 S. Grimme, J. Antony, S. Ehrlich and H. Krieg, *J. Chem. Phys.*, 2010, **132**, 154104.
28 S. Grimme, S. Ehrlich and L. Goerigk, *Journal of Computational Chemistry*, 2011, **32**, 1456–1465.
29 N. Mehta, M. Casanova-Páez and L. Goerigk, *Phys. Chem. Chem. Phys.*, 2018, **20**, 23175–23194.
30 F. Weigend and R. Ahlrichs, *Phys. Chem. Chem. Phys.*, 2005, **7**, 3297–3305.
31 L. Goerigk, A. Hansen, C. Bauer, S. Ehrlich, A. Najibi and S. Grimme, *Phys. Chem. Chem. Phys.*, 2017, **19**, 32184–32215.
32 F. Neese, *WIREs Computational Molecular Science*, 2018, **8**, e1327.
33 M. Cossi, N. Rega, G. Scalmani and V. Barone, *J. Chem. Phys.*, 2001, **114**, 5691–5701.
34 F. Weigend, A. Köhn and C. Hättig, *J. Chem. Phys.*, 2002, **116**, 3175–3183.
35 J. J. Snellenburg, S. Laptenok, R. Seger, K. M. Mullen and I. H. M. van Stokkum, *Journal of Statistical Software*, 2012, **49**, 1–22.

View Article Online
DOI: 10.1039/D1CP00541C

36 M. Kirkus, R. A. J. Janssen and S. C. J. Meskers, *J. Phys. Chem. A*, 2013, **117**, 4828–4837.

37 M. Kirkus, L. Wang, S. Mothy, D. Beljonne, J. Cornil, R. A. J. Janssen and S. C. J. Meskers, *J. Phys. Chem. A*, 2012, **116**, 7927–7936.

38 M. Gora, S. Pluczyk, P. Zassowski, W. Krzywiec, M. Zagorska, J. Mieczkowski, M. Lapkowski and A. Pron, *Synthetic Metals*, 2016, **216**, 75–82.

39 M. Gora, W. Krzywiec, J. Mieczkowski, E. C. Rodrigues Maia, G. Louarn, M. Zagorska and A. Pron, *Electrochimica Acta*, 2014, **144**, 211–220.

40 B. Barszcz, K. Kędzierski, H. Y. Jeong and T.-D. Kim, *Journal of Luminescence*, 2017, **185**, 219–227.

41 A. Aster, G. Licari, F. Zinna, E. Brun, T. Kumpulainen, E. Tajkhorshid, J. Lacour and E. Vauthey, *Chem. Sci.*, 2019, **10**, 10629–10639.

42 A. Aster, F. Zinna, C. Rumble, J. Lacour and E. Vauthey, *J. Am. Chem. Soc.*, 2021.

43 E. A. Buchanan, Z. Havlas and J. Michl, *Advances in Quantum Chemistry*, Academic Press, 2017, vol. 75, pp. 175–227.

44 D. Beljonne, H. Yamagata, J. L. Brédas, F. C. Spano and Y. Olivier, *Phys. Rev. Lett.*, 2013, **110**, 226402.

45 R. D. Pensack, A. J. Tilley, C. Grieco, G. E. Purdum, E. E. Ostroumov, D. B. Granger, D. G. Oblinsky, J. C. Dean, G. S. Doucette, J. B. Asbury, Y.-L. Loo, D. S. Seferos, J. E. Anthony and G. D. Scholes, *Chem. Sci.*, 2018, **9**, 6240–6259.